

Photoluminescent and Electroluminescent Zn₂Si_{0.5}Ge_{0.5}O₄:Mn Thin Films for Integrated Optic Devices

Christopher C. Baker, *Student Member, IEEE*, Jason Heikenfeld, *Member, IEEE*, and Andrew J. Steckl, *Fellow, IEEE*

Abstract—The optical, photoluminescent (PL), and electroluminescent (EL) properties of Zn₂Si_{0.5}Ge_{0.5}O₄:Mn (ZSG:Mn) have been studied in order to determine its viability as a light source for integrated optics systems. ZSG:Mn thin films were deposited at room temperature by RF-sputtering on Si substrates. EL devices (ELDs) were fabricated using transparent indium-tin oxide electrodes. ELDs using as-deposited ZSG:Mn films emitted bright orange light with a broad spectrum at 590–660 nm. Annealing at 700 °C resulted in a color shift to green emission in a band from 510 to 550 nm and peaking at 520 nm. Ridge waveguides fabricated by induction-coupled plasma etching yielded an optical loss of 3.8 dB/cm at 633 nm. Prism coupling experiments revealed a decrease in the film refractive index as the result of the anneal. The combination of strong PL, EL, and low waveguide loss demonstrates the strong potential of transition metal- and/or rare-earth-doped ZSG as a robust light source for integrated optic systems.

Index Terms—Electroluminescence, manganese, optical code division multiple access (OCDMA), optical waveguides, photoluminescence, prism coupling, zinc silicate germanate.

I. INTRODUCTION

RECENTLY there has been a great deal of progress in oxide thin-film phosphors for electroluminescent displays. Alternating current (ac) electroluminescent devices (ELDs) achieving 180 cd/m² at a 60-Hz refresh rate have been reported [1] in sputtered Mn-doped Zn₂Si_{0.5}Ge_{0.5}O₄ (ZSG) films. Very high ELD efficiency of 10 lm/W has been reported [2] for (Y₂O₃)_{1-x}(GeO₂)_x:Mn thin-film oxide phosphors. Furthermore, strong photoluminescence (PL) in Zn₂SiO₄ doped with rare earths such as Eu³⁺ and Tb³⁺ has also been reported [3]. The combination of intense electroluminescence (EL), the potential to incorporate a variety of transition metal and rare-earth dopants and high optical transparency has led us to consider the zinc silicate-germanate (ZSG) material system as a light source for integrated optics applications. Initial investigations reported here quickly revealed that the room-temperature sputtered material had excellent waveguiding properties. This work demonstrates the initial feasibility of integrating EL devices and optical waveguides using the ZSG:Mn (and similar) material systems. The broad EL emission band, characteristic of transition metal dopants in phosphors,

will be useful in a future optical code division multiple access (OCDMA) communication system. Furthermore, the most prevalent plastic optical fiber has its attenuation minimum in the red, a wavelength region of strong emission in as-deposited ZSG:Mn thin films.

In Section II, we present the PL and EL properties of ZSG:Mn, which reveal the existence of broad spectral peaks that may be shifted in the visible regime as a function of annealing temperature. Section III contains the evaluation of the ZSG:Mn refractive index as a function of annealing temperature, utilizing the prism coupling technique. This method not only provides the film refractive index and thickness, but also gives insight into any index gradients and nonuniformity by comparing the propagation constant n_e with the theoretical value based on a fixed index. Section IV presents the fabrication of channel waveguides through inductively coupled plasma (ICP) etching and gives the results of initial loss measurements. Section V discusses the potential system applications of the ZSG:Mn components.

II. PL AND EL

ZSG:Mn films were deposited on 4-in bare Si wafers for EL measurements and on oxidized Si wafers with a 2.5- μ m thermal oxide to act as a lower cladding for planar and channel waveguide structures. The films were deposited at room temperature using a Denton Discovery 18 sputtering system. The films were RF sputtered from a 99.9% Zn_{1.96}Si_{0.5}Ge_{0.5}O₄:Mn_{0.04} target supplied by SCI Engineered Materials Inc. The sputtering conditions were 250 W (\sim 5.5 W/cm²), 40 sccm Ar, 3 sccm Ar/O mix (80:20), 5 mTorr, and a plasma-induced dc bias of -285 V. The three-cathode system is set up in a confocal configuration with a target center to a substrate center distance of \sim 10 cm and a target angle optimized for $< 5\%$ film thickness variation. The 6-in substrate platen was rotated at 12 rpm. Films were sputtered at a rate of \sim 12.5 nm/min, which yielded \sim 1.5 μ m films after 120 min of sputtering. Sputtering of the films at elevated substrate temperature (350 °C) produced increased optical scattering in the films. An SEM cross section of the planar waveguiding structure is given in Fig. 1. We use the convention of naming the indices of refraction of various layers as follows: n_1 for air, n_2 for the ZSG:Mn layer, and n_3 for the SiO₂ layer. Selected films were furnace annealed in an N₂ atmosphere for 90 min primarily at a temperature of 700 °C. X-ray diffraction (XRD) analysis revealed that a 700 °C anneal results in the formation of polycrystalline ZSG, as can

Manuscript received September 4, 2002; revised October 1, 2002. This work was supported by an ARO grant.

C. C. Baker and A. J. Steckl are with the Nanoelectronics Laboratory, University of Cincinnati, Cincinnati, OH 45221-0030 USA.

J. Heikenfeld is with the Extreme Photonix LLC, Cincinnati, OH 45219-2374 USA.

Digital Object Identifier 10.1109/JSTQE.2002.806695



Fig. 1. SEM photomicrograph showing the cross section of a ZSG:Mn planar waveguiding structure.

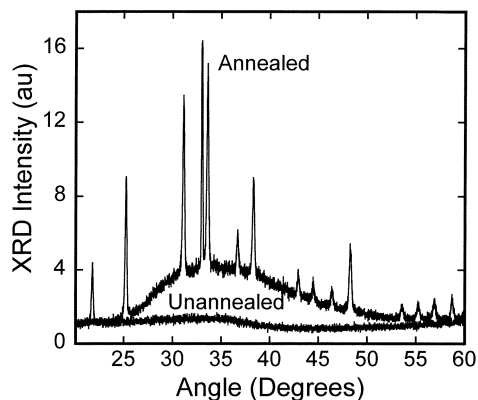


Fig. 2. XRD spectrum of as-deposited and annealed (700 °C) ZSG:Mn.

be seen in Fig. 2. Prominent ZSG peaks are clearly visible in the annealed sample while none are present in the unannealed sample. The peaks are attributed solely to the ZSG:Mn layer since the underlying amorphous SiO_2 layer is much thicker than the XRD penetration capability. The surface roughness, measured by atomic force microscopy, was 3.63 nm for the as-deposited film and 1.86 nm for the annealed film.

ZSG:Mn PL was measured using a 325-nm He–Cd laser for excitation. This pump wavelength is not within the peak efficiency pumping spectrum [4] found at 200–300 nm for $\text{Zn}_2\text{SiO}_4:\text{Mn}$, but the ZSG:Mn PL signal is still very intense and is fully adequate for PL characterization. The emission spectra were analyzed by an Acton Research spectrometer equipped with a photomultiplier sensitive in the UV-visible spectrum. All PL measurements were performed at 300 K. PL spectra for unannealed and annealed samples are shown in Fig. 3. The two components of ZSG, $\text{Zn}_2\text{SiO}_4:\text{Mn}$ and $\text{Zn}_2\text{GeO}_4:\text{Mn}$, are known to exhibit [5] broad emission bands, peaking at 525 and 537 nm, respectively. The PL from the as-deposited sample contains two multiplex bands in the blue (from ~ 390 to 450 nm) and in the yellow–red region (from ~ 560 to 680 nm). Annealing at 700 °C results in PL emission from two closely spaced peaks at 524 and 542 nm. After annealing at 800 °C, a single PL peak at 531 nm is observed.

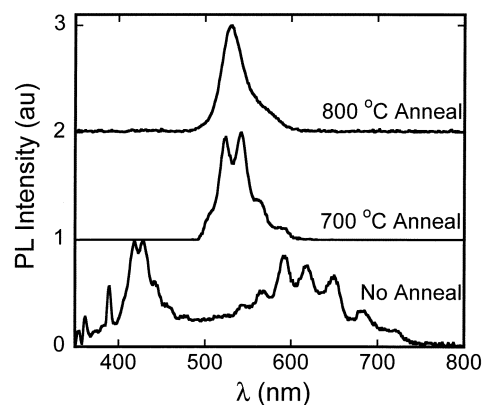


Fig. 3. PL spectra for the as-deposited and annealed (700 °C, 800 °C) ZSG:Mn films.

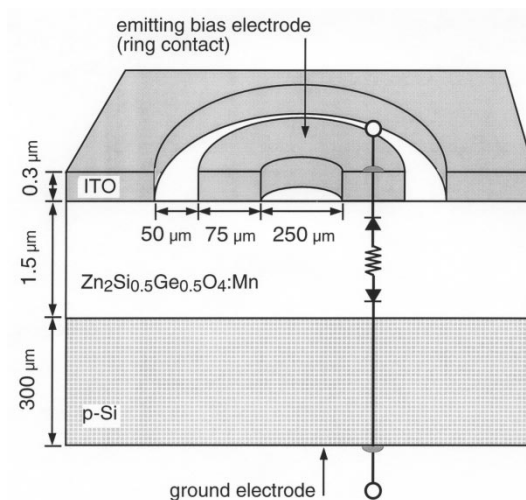


Fig. 4. Schematic diagram of the ELD structure.

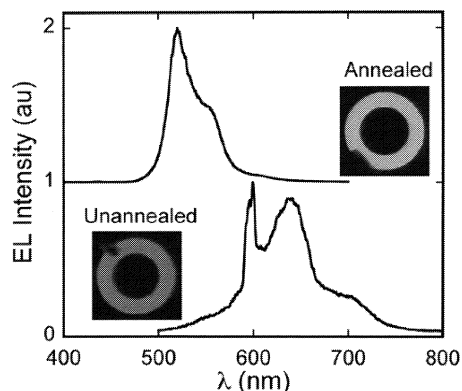


Fig. 5. EL spectra for the annealed and unannealed ZSG:Mn devices.

A dc ELD was utilized to characterize EL emission. The device structure shown in Fig. 4 uses a ring electrode for the bias electrode and therefore emission area. A detailed description of the ring ELD fabrication sequence has been previously reported [6]. The EL spectra for both unannealed and 700 °C annealed devices (along with corresponding photographs of EL emission) are shown in Fig. 5. EL emission occurs and was measured just above the onset of electrical breakdown (~ 2 MV/cm) of

the ZSG:Mn layer. DC ELD operation was stable up to catastrophic electrical breakdown at ~ 3 MV/cm operation. The Mn excitation method in ELDs is impact excitation by hot electrons (> 2 eV) generated by the high applied field. With proper EL device design, excitation might originate from other sources such as electron-hole-based recombination (p-n or p-i-n junction). However, impact excitation mediated EL alone can deliver high efficiency (~ 1 lm/W) from an ac-ELD device [1] using a ZSG:Mn layer. A strong shift of the emission spectrum was measured between the unannealed EL device (red emission) and 700 °C annealed EL device (green emission). These results are consistent with the spectra measured from alternating current ELD ZSG:Mn devices [7]. The red emission from the unannealed ELD is produced by two peaks at 600 and 635 nm. The green emission from the 700 °C annealed ELD is due to a single broad line with a peak at ~ 520 nm. This peak is also observed by PL excitation. However, the second PL peak at 542 nm (see Fig. 3) is either not produced in EL excitation or is much reduced (and contained in the shoulder of the primary peak). The shift of EL emission from red to green with annealing is attributed to a decrease in crystal field [8] strength due to the crystallization of the ZSG host. This leads to a decrease in splitting of the $3d^5$ configuration and therefore increased energetic spacing between the light emissive ${}^4T_1 - > {}^6A_1$ energy level transition of Mn^{2+} .

It should be noted that most ELD structures are inherently optical waveguides because of the high refractive index of the emissive layer. ELDs are most commonly utilized for flat panel display applications. In EL displays [9], the light out-coupling efficiency is only $\sim 5\%$ - 10% . Although this is a disadvantage for display usage, this effect is ideal for integrated optic systems. Use of an ELD device as a lateral emitter [10] can yield light intensities so strong that such devices were developed by several groups as a linear array light source [9] for electrophotographic printer applications. However, for integrated optic usage, a key additional attribute is required, namely high optical transparency for waveguiding, a topic discussed in the next sections.

III. EVALUATION OF THE REFRACTIVE INDEX

The refractive index of ZSG:Mn has been evaluated using the prism coupling method [11]. The refractive index was measured at 632.8 and 1553.3 nm. A Metricon Corporation 2010 Model 2010 prism coupler with multiwavelength capabilities, which can measure the properties of both the waveguide core and cladding, was used to evaluate the planar waveguide structures. To achieve prism coupling it is necessary that the components of the phase velocities of the waves in the propagation direction be the same in both the waveguide and the beam. This requires that a phase-matching condition be satisfied [12]. The condition is met when the following relation between the wave propagation constants and the angle of incidence can be satisfied:

$$\beta_m = kn_p \sin \theta_m \quad (1)$$

where

$$k = \frac{2\pi}{\lambda_0} \quad (2)$$

$$\beta = kn_e. \quad (3)$$

n_p is the refractive index of the prism, n_e is the effective index, λ_0 is the free space wavelength, and θ_m is the angle of the incident light relative to the axis normal to the prism base. The refractive index and film thickness are determined by minimizing the error sum

$$\sigma(n, kW) = \sum_m \left[\tilde{\beta}_m - \beta_m(n, kW) \right]^2 \quad (4)$$

where $\tilde{\beta}_m$ are the observed propagation constants, $\beta_m(n, kW)$ are the solutions of the dispersion equation for a given combination of film index and thickness, W is the physical width of the core layer, and m is the mode index.

The unannealed ZSG:Mn sample had a higher than expected standard deviation in the evaluation of the film refractive index and thickness. The standard deviation of between 1.5% and 2.0% for the film thickness was found by utilizing the fact that having more than two propagating modes for a planar waveguide structure results in an overdetermined solution, thus providing a self-consistent mechanism for evaluating error. The presence of this high standard deviation is thought to be the result of an index gradient in the film [13] and made it necessary to use an assumed value for the SiO_2 cladding layer instead of doing a dual-film analysis. The index gradient is likely the result of film stress. The refractive index and thickness of the ZSG film was measured by evaluating both the TE and TM modes. Using only the TE modes, the refractive index of the unannealed ZSG was found to be ~ 1.77 and ~ 1.74 with thicknesses of 1.47 and 1.5 μm at wavelengths of 632.8 and 1553.3 nm, respectively. Using TM mode evaluation, the refractive index was found to be 1.77 and 1.74 with thicknesses of 1.48 and 1.51 μm at the same wavelengths of 632.8 and 1553.3 nm, respectively. The slightly thicker film measurements for the TM analysis are likely a result of overcoupling, so the film thickness and refractive index measured using TE modes at 632.8 nm were used to construct a dispersion diagram.

Dispersion diagrams are useful in determining whether the experimentally observed propagation constants β or n_e match those given by a theoretical evaluation based solely on refractive index and thickness. Following Boyd [14], the dispersion diagrams are generated by numerically solving the constraint equation

$$\tan ht = \frac{\sigma_2(\sigma_3p + \sigma_1q)}{(\sigma_2h) - \sigma_1\sigma_3pq} \quad (5)$$

where

$$\begin{aligned} p &= k(n_2^2 - n_e^2)^{1/2} \\ q &= k(n_e^2 - n_1^2)^{1/2} \\ h &= k(n_e^2 - n_3^2)^{1/2} \end{aligned} \quad (6)$$

and σ_i is 1 for TE modes and $1/n_i^2$ for the TM modes. The subscript i is the layer index and the values m represent the

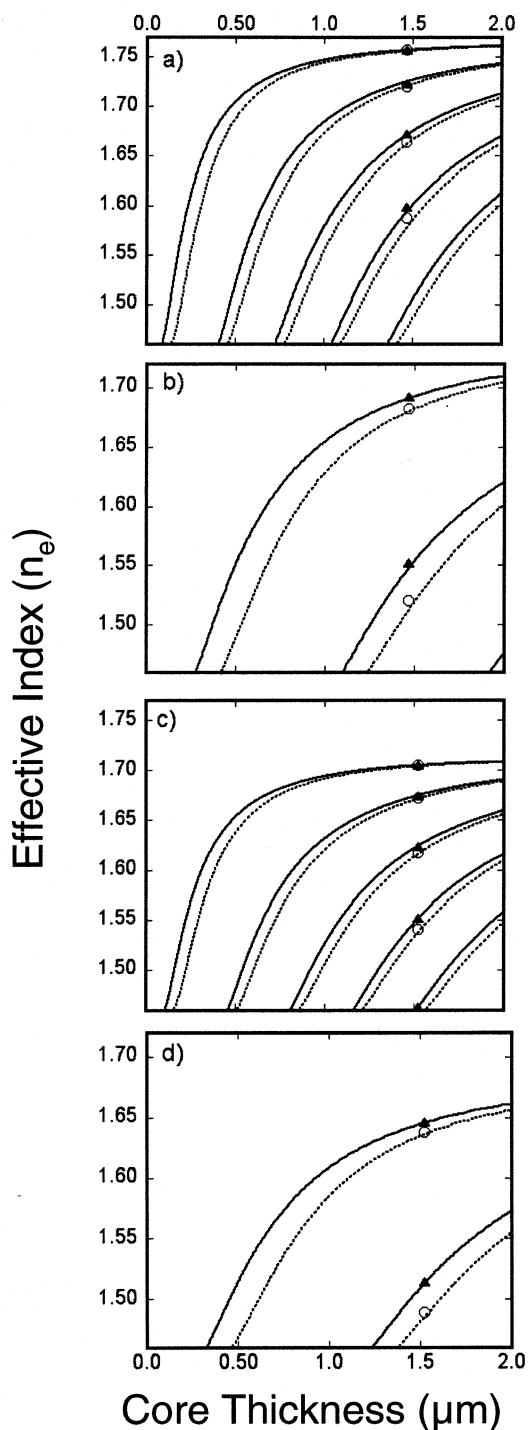


Fig. 6. Dispersion diagrams for ZSG:Mn planar waveguides. (a) As-deposited film at 632.8 nm. (b) As-deposited film at 1553.3 nm. (c) A 700 °C annealed film at 632.8 nm. (d) A 700 °C annealed film at 1553.3 nm. The individual data symbols are experimental values obtained using the prism coupling technique.

mode number. Solutions are found by iterating n_e between a value just above n_3 to a value just below n_2 . The dispersion diagrams for the unannealed waveguide samples are given in Fig. 6. The theoretical and experimental results at 632.8 nm are given in (a) and those taken at 1550 nm in (b).

The ZSG:Mn sample annealed at 700 °C yielded more consistent results in the prism coupling analysis, indicating that the anneal removed the refractive index gradient. The

smaller standard deviation allowed us to measure both the core and cladding refractive indices and thickness. In all cases, the annealing process produced a lower refractive index. The calculated and measured effective indices for the annealed ZSG:Mn film at 632.8 and 1553.3 nm are given in Fig. 6(c) and (d), respectively. At 632.8 nm using TE modes, the analysis yielded a refractive index of 1.72 and a film thickness of 1.52 μm for the core layer and corresponding values of 1.46 and 2.5 μm for the SiO_2 cladding. At a wavelength of 1553.3 nm, the core refractive index and thickness were 1.69 μm and 1.533 μm , respectively, with a cladding refractive index of 1.45 and a thickness of 2.42 μm . As mentioned above, the thinner cladding layer measurement in the infrared is thought to be the result of overcoupling, therefore the measurement at 632.8 nm is probably more accurate. Using the TM modes, slightly higher refractive indices of 1.72 and 1.69 at 632.8 and 1553.3 nm, respectively, are likely to be correct. The thickness of 1.53 μm at 632.8 nm and 1.54 μm at 1553.3 nm were measured. The measured results for the annealed and unannealed films are summarized in Table I.

IV. CHANNEL WAVEGUIDE FABRICATION AND LOSS MEASUREMENTS

ZSG:Mn channel waveguides were fabricated using Cl_2/Ar -based inductively coupled plasma (ICP) etching. This work was conducted using a PlasmaTherm 790 plasma reactor operated in the inductively coupled plasma (ICP) mode. The etch mask used consisted of a 1.8- μm -thick layer of Shipley 1818 positive photoresist. An ICP power of 500 W and an RF power of 100 W were found to give acceptable initial results for waveguide testing and material evaluation. The gas flow rates were 15 sccm Cl_2 and 5 sccm Ar. An SEM photograph of a typical waveguide is shown in Fig. 7. It was found that the material etched fairly slowly. This was not surprising, however, as the material is highly insulating. Further study is needed to find the optimum etching parameters for this material.

Optical characterization of channel waveguides was performed using the outscattering technique [15]. The waveguide loss measurement setup consists of one of several laser sources, a focusing lens and microscope having a Gamma Scientific model 700-10-40A eyepiece with optical fiber pickup. An 8 \times (0.15 N.A.) long working distance objective was used to collect the outscattered light from the propagating modes. The collected light is focused into a 3-mm-diameter fiber probe conveying it to a photomultiplier tube. An infrared camera connected to a monitor is used to observe the waveguiding channels. Scattering from the input edge of the waveguide was avoided by taking the measurement far from the input. Excellent facets for end fire coupling were easily achieved due to the cleaving characteristics of $\langle 100 \rangle$ Si substrates. An unannealed ZSG:Mn waveguide ($\sim 5 \mu\text{m}$) propagating 632.8 nm light is shown in Fig. 8. The completely black square in the center of the waveguide is the shadow of the fiber-optic pick-up. Coupling into adjacent waveguides and scattering from pinholes is clearly visible. The defect density is expected to decrease dramatically after further optimizing the sputtering conditions. The results from a typical 5- μm ZSG:Mn waveguide are given

TABLE I
ZSG:Mn REFRACTIVE INDEX AND THICKNESS MEASUREMENTS USING THE PRISM COUPLING METHOD

Anneal	Wavelength (μm)	Polarization	ZSG:Mn Refractive Index (n)	ZSG:Mn Thickness (μm)	SiO ₂ Refractive Index (n)	SiO ₂ Thickness (μm)
None	0.6328	TE	1.77 (SD=0.02%)	1.47 (SD=1.76%)		
None	0.6328	TM	1.77 (SD=0.02%)	1.48 (SD=1.45%)		
None	1.5533	TE	1.74	1.5		
None	1.5533	TM	1.74	1.51		
700°C	0.6328	TE	1.72 (SD=0.01%)	1.52 (SD=0.53%)	1.46 (SD=0.004%)	2.5 (SD=0.417%)
700°C	0.6328	TM	1.72 (SD=0.01%)	1.53 (SD=0.43%)		
700°C	1.5533	TE	1.69	1.53	1.45	2.42
700°C	1.5533	TM	1.69	1.54		

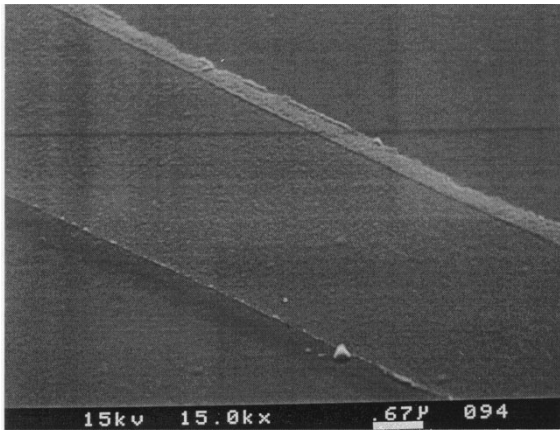


Fig. 7. SEM photomicrograph of a ZSG:Mn channel waveguide fabricated by inductively coupled plasma etching.

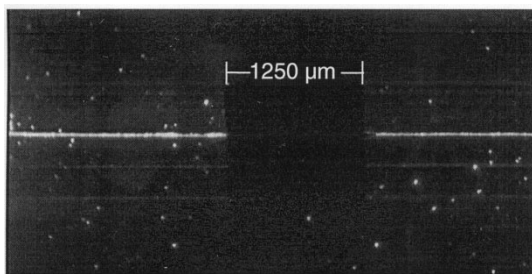


Fig. 8. ZSG:Mn waveguide propagating 632.8 nm light.

in Fig. 9, showing a loss of 3.8 dB/cm. While this loss is high when compared to silica waveguides, it is of the same order of magnitude as semiconductor waveguide structures. Losses of less than 1 dB/cm are expected to be achieved when sputtering conditions, lithographic techniques, and etching are optimized, making ZSG:Mn a viable material for ZSG:Mn integrated optics.

Planar and channel waveguides fabricated using annealed ZSG:Mn exhibited much higher loss. It is possible that the

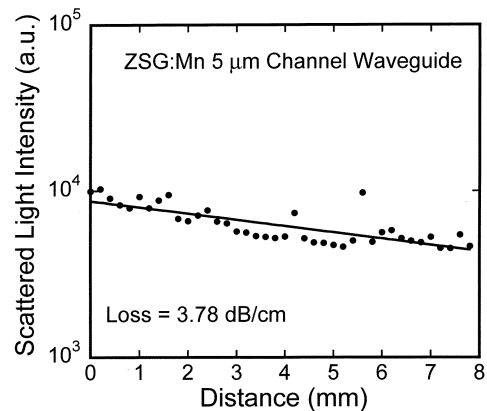


Fig. 9. Channel loss in a typical 5- μm ZSG:Mn waveguide at 632.8 nm.

annealing process resulted in an inhomogeneous polycrystalline structure, which provided effective scattering centers. Functional waveguides on annealed ZSG:Mn requires further study of the annealing process and possibly the use of other deposition techniques (such as atomic layer epitaxy) which can provide good crystallinity and light guiding capability.

V. POTENTIAL APPLICATIONS

OCDMA communication systems have been shown to be very valuable in a wide range of systems including wireless, LAN, and metro applications. Traditional OCDMA systems rely on encoding the information signal in the time domain by a pseudorandom sequence. While this proves efficient, the need for longer code lengths as the number of simultaneous users increases, without sacrificing performance, necessitates shorter and shorter pulses. These systems must rely on mode-locked lasers making the scheme too expensive to compete with other access schemes [16].

Frequency-encoded OCDMA (FE-OCDMA) systems have been proposed which relax the constraints on pulse length by using noncoherent broad-band optical sources and spectral

encoding to add another coding dimension [16], [17]. We propose a new integrated optic system incorporating a broad-band ZSG:Mn light source and arrayed waveguide gratings on a single chip to achieve spectral spreading without using complicated epitaxy or flip-chip bonding techniques [18] and eliminating the need for bulk optics and diffraction gratings. The devices may either be “hard-coded” to produce a single optical code or incorporated into a dynamic system.

While the visible spectrum is not useful in conventional optical communication systems, it is commonly used in plastic optical fiber (POF). The reported attenuation minima for polymethylmethacrylate (PMMA) optical fibers are at 570 and 650 nm [19]. It is believed that emission at both of these wavelengths is easily achieved using the ZSG:Mn material system by adjusting anneal time and temperature. POFs have shown themselves to be very inexpensive and useful in a variety of applications [20], [21]. The proposed spectral encoding system has the potential to be much less expensive than previously proposed OCDMA systems and have a smaller parts count.

VI. SUMMARY

The optical properties of zinc silicate-germanate films doped with Mn have been investigated for integrated optics applications. Strong EL emission was observed in the red region of the spectrum for as-deposited ZSG:Mn films. Upon anneal a shift to green emission was observed. Ridge waveguides were fabricated using plasma-assisted etching. Channel loss of 3.8 dB/cm was measured at a wavelength of 633 nm. Prism coupling was utilized to measure the refractive index at 633 nm and 1.5 μm . We anticipate that robust light sources for selected wavelengths can be fabricated using ZSG layers doped with a combination of rare earths and transition metals.

ACKNOWLEDGMENT

The authors would like to thank J. Jackson of Metricon for providing the refractive index measurements. The authors would like to acknowledge the support and encouragement of J. Zavada.

REFERENCES

- [1] A. K. Kitai, “Oxide phosphor green EL devices on glass substrates,” *Proc. SID 99 Digest*, pp. 596–598, 1999.
- [2] T. Minami, Y. Kobayashi, T. Miyata, and S. Suzuki, “High luminance thin-film electroluminescent devices using $(Y_2O_3)_{0.6}-(GeO_2)_{0.4}$:Mn phosphors,” *Jpn. J. Appl. Phys.*, vol. 41, pp. 577–579, 2002.
- [3] H. X. Zhang, S. Buddhudu, C. H. Kam, Y. Zhou, Y. L. Lam, K. S. Wong, B. S. Ooi, S. L. Ng, and W. X. Que, “Luminescence of Eu^{3+} and Tb^{3+} doped Zn_2SiO_4 nanometer powder phosphors,” *Mat. Chem. Phys.*, vol. 68, pp. 31–35, 2001.
- [4] S. Kamiya and H. Mizuno, “Phosphors for lamps,” in *Phosphor Handbook*, S. Shionoya and W. M. Yen, Eds. Boca Raton, FL: CRC Press, 1999, ch. 5, sec. 6.
- [5] S. Tanimizu, “Principal phosphor materials and their optical properties,” in *Phosphor Handbook*, S. Shionoya and W. M. Yen, Eds. Boca Raton, FL: CRC Press, 1999, ch. 3, sec. 3.2.5.1.
- [6] M. Garter, J. Scofield, R. Birkhahn, and A. J. Steckl, “Visible and infrared rare-earth-activated electroluminescence from indium tin oxide Schottky diodes to GaN:Er on Si,” *Appl. Phys. Lett.*, vol. 74, no. 2, pp. 182–184, Jan. 1999.

- [7] A. Kitai, T. Xiao, and G. Liu, “,” U.S. Patent #5 725 801, 1998.
- [8] G. Blasse and B. C. Grabmaier, *Luminescent Materials*. Berlin, Germany: Springer Verlag, 1994.
- [9] R. Mueller-Mach and G. O. Mueller, “Thin film electroluminescence,” in *Electroluminescence II, Semiconductors and Semimetals*, G. O. Mueller, Ed. San Diego, CA: Academic, 2000, vol. 65, ch. 2.
- [10] M. R. Craven, W. M. Cranton, S. Toal, and H. S. Reehal, “Characterization of $BaTiO_3$ thin films deposited by RF magnetron sputtering for use in a.c. TFEL devices,” *Semicond. Sci. Technol.*, vol. 13, pp. 404–409, 1998.
- [11] P. Ulrich and R. Torge, “Measurement of thin film parameters with a prism coupler,” *Appl. Opt.*, vol. 12, no. 12, pp. 2901–2908, 1973.
- [12] R. G. Hunsperger, *Integrated Optics: Theory and Technology*. Berlin, Germany: Springer-Verlag, 1991.
- [13] D. Ciplys, R. Gaska, and M. S. Shur, “Propagation of guided optical waves in thick GaN layers grown on (0001) sapphire,” *Appl. Phys. Lett.*, vol. 76, no. 16, pp. 2232–2234.
- [14] J. T. Boyd, *Photonic Devices and Systems*, R. G. Hunsperger, Ed. New York: Marcel Dekker, 1994, ch. 9, pp. 313–375.
- [15] V. Subramaniam, G. N. DeBrabander, D. H. Nagski, and J. T. Boyd, “Measurement of mode field profiles and bending and transition losses in curved optical channel waveguides,” *J. Lightwave Technol.*, vol. 15, pp. 990–997, June 1997.
- [16] M. Kavehrad and D. Zaccarain, “Optical code-division-multiplexed systems based on spectral encoding of noncoherent sources,” *J. Lightwave Technol.*, vol. 13, pp. 534–545, Mar. 1995.
- [17] N. Karafolas and D. Uttamchandani, “Optical fiber CDMA networks,” *Opt. Fiber Technol.*, vol. 2, pp. 149–168, 1996.
- [18] R. Wirth, C. Karnutsch, S. Kugler, and K. Streubel, “High-efficiency resonant-cavity LED’s emitting at 650 nm,” *IEEE Photon. Technol. Lett.*, vol. 13, pp. 421–423, May 2001.
- [19] A. Neyer, B. Wittmann, and M. Johnck, “Plastic-optical-fiber-based parallel optical interconnects,” *IEEE J. Select. Topics Quantum Electron.*, vol. 5, pp. 193–200, Mar./Apr. 1999.
- [20] Y. Koike, T. Ishigure, and E. Nibei, “High-bandwidth graded-index polymer optical fiber,” *J. Lightwave Technol.*, vol. 13, pp. 1475–1489, July 1995.
- [21] Z. Xiong, G. D. Peng, B. Wu, and P. L. Chu, “Highly tunable Bragg gratings in single-mode polymer optical fibers,” *IEEE Photon. Technol. Lett.*, vol. 11, pp. 352–354, Mar. 1999.



Christopher C. Baker (S’00) received the B.S. degree in physics from Miami University, Oxford, OH, in 1998. His undergraduate research was in the field of giant magnetoresistance for which he received funding through Miami University’s Undergraduate Summer Scholar program.

Upon graduation he began his Ph.D. studies in electrical engineering at the University of Cincinnati where he focused on active and passive integrated optic components. In 2001 he joined the Nanoelectronics Laboratory as a Research Associate to

develop novel GaN photonic devices.

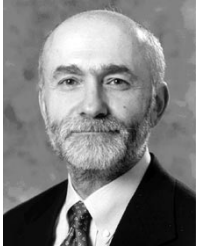
Mr. Baker is a member of the Optical Society of America and the Materials Research Society.



Jason Heikenfeld (S’99–M’03) received the B.S. and Ph.D. degrees in electrical engineering from the University of Cincinnati, Cincinnati, OH, in 1998 and 2001, respectively. His doctoral research concentrated on novel inorganic electroluminescent display devices based on rare earth-doped GaN.

He is now a Research Scientist at Extreme Photonix LLC, Cincinnati. His main duties at Extreme Photonix involve leading the development of electroluminescent devices for flat panel displays. He has authored and coauthored 30 publications on photonic materials and devices in refereed journals, conference proceedings, and a book chapter. He is an inventor on three pending U.S. patents.

Dr. Heikenfeld is a member of the Society for Information Display, the Materials Research Society, and the American Society for Engineering Education.



Andrew J. Steckl (S'70–M'73–SM'79–F'99) received the B.S.E. degree in electrical engineering from Princeton University, Princeton, NJ, in 1968 and the M.Sc. and Ph.D. degrees from the University of Rochester, Rochester, NY, in 1970 and 1973, respectively.

In 1972, he joined the Honeywell Radiation Center, Lexington, MA, as a Senior Research Engineer, where he worked on new concepts and devices in the area of infrared detection. In 1973, he joined the Technical Staff of the Electronics

Research Division of Rockwell International, Anaheim, CA. At Rockwell he was primarily involved in research on charge coupled devices. In 1976, he joined the Electrical, Computer and Systems Engineering Department at Rensselaer Polytechnic Institute, Troy, NY, where he developed a research program in microfabrication of Si devices. In 1981, he founded the Center for Integrated Electronics, a multidisciplinary academic center focused on VLSI research and teaching, and served as its director until 1986. In 1988, he joined the Electrical and Computer Engineering Department of the University of Cincinnati, Cincinnati, OH, as Ohio Eminent Scholar and Gieringer Professor of Solid State Microelectronics. At Cincinnati he has built the Nanoelectronics Laboratory with research activities in semiconductor materials and devices for photonics: SiC and GaN thin-film growth by CVD and MBE, focused ion beam fabrication of photonic components and circuits, rare-earth-doped luminescent devices for flat panel displays and communications. His research has resulted in over 290 publications and 300 conferences and seminar presentations.